Electronic Supplementary Material (ESI) for Journal of Materials Chemistry

SUPPORTING INFORMATION

A First-Principles Study of II-VI (II = Zn; VI = O, S, Se, Te) Semiconductor Nanostructures

Jon M. Azpiroz,[*,a] Ivan Infante,[a] Xabier Lopez[a] and Jesus M. Ugalde[a]

[a]Kimika Fakultatea, Euskal Herriko Unibertsitatea (UPV/EHU) and Donostia International Physics Center (DIPC), P.K. 1072 Donostia, Euskadi, Spain

Filippo De Angelis[b]

[b]Istituto CNR di Science e Tecnologie Molecolari (ISTM-CNR), c/o Dipartimento di Chimica, Università degli Studi di Perugia, Via Elce di Sotto 8, I-06123, Perugia, Italy

Table 1: Geometric parameters of the ZnS-NR1 optimized at different levels. Bond lengths and angles are given. The numbers in parentheses mean the coordination number of each atom. Notice that Zn-S bond lengths are only 0.01 Å shorter at PBE/DZ as compared to B3LYP/DZ. Likewise, the bond angles are quite similar. The structure changes only slightly when the implicit solvent is introduced, irrespective of the functional. Moreover, it seems that the polarity of the solvent plays a minor role.

	B3LYP/DZ	COSMO(water)-B3LYP/DZ	PBE/DZ	COSMO(water)-PBE/DZ	COSMO(acetonitrile)-PBE/DZ
d(Zn(2)-S)	2.294	2.303	2.294	2.300	2.299
d(S(2)-Zn)	2.313	2.346	2.300	2.330	2.326
d(Zn(3)-S)	2.433	2.425	2.418	2.410	2.411
d(S(3)-Zn)	2.432	2.424	2.418	2.410	2.412
α(S-Zn(2)-S)	161.9	152.7	163.6	155.6	155.3
α(Zn-S(2)-Zn)	82.8	84.6	81.9	83.9	84.1
α(S-Zn(3)-S)	116.5	117.4	117.5	118.3	118.4
α(Zn-S(3)-Zn)	95.5	96.6	93.7	94.8	94.8

Table 2: Electronic parameters calculated for the ZnX-NRs (X = S, Se, Te), in eV. d is the position of the d peak. ε_{HOMO-1}, ε_{HOMO}, ε_{LUMO}, and ε_{LUMO+1} are the HOMO-1, HOMO, LUMO and LUMO+1 KS eigenvalues, respectively. $\triangle_d$ refers to the binding energy of the d peak, taken with respect to the VBM (the HOMO-1 in our case). $\triangle_{HOMO-LUMO}$, $\triangle_{HOMO-1-LUMO}$ and $\triangle_{LUMO-LUMO+1}$ are the HOMO-LUMO, HOMO-1-LUMO and LUMO-LUMO+1 energy gaps. Results obtained at PCM-B3LYP/def2-SVP//PBE/DZ.

ZnS	d	ε_{HOMO-1}	ε_{HOMO}	ε_{LUMO}	ε_{LUMO+1}	$\triangle_d$	$\triangle_{HOMO-LUMO}$	$\triangle_{HOMO-1-LUMO}$	$\triangle_{LUMO-LUMO+1}$
NR1	-14.80	-6.78	-6.21	-1.24	-0.64	8.02	4.97	5.54	0.60
NR2	-14.76	-6.77	-6.20	-1.28	-0.93	7.99	4.92	5.49	0.35
NR3	-14.75	-6.71	-6.20	-1.30	-1.08	8.04	4.90	5.41	0.22
NR4	-14.73	-6.65	-6.20	-1.28	-1.14	8.08	4.92	5.37	0.14
NR5	-14.72	-6.63	-6.20	-1.30	-1.19	8.09	4.90	5.33	0.11

ZnSe	d	ε_{HOMO-1}	ε_{HOMO}	ε_{LUMO}	ε_{LUMO+1}	$\triangle_d$	$\triangle_{HOMO-LUMO}$	$\triangle_{HOMO-1-LUMO}$	$\triangle_{LUMO-LUMO+1}$
NR1	-14.97	-6.64	-6.08	-1.31	-0.77	8.33	4.77	5.33	0.54
NR2	-14.93	-6.51	-6.07	-1.34	-1.02	8.42	4.73	5.17	0.32
NR3	-14.91	-6.42	-6.07	-1.35	-1.15	8.49	4.72	5.07	0.20
NR4	-14.90	-6.37	-6.06	-1.36	-1.22	8.53	4.70	5.01	0.14
NR5	-14.89	-6.35	-6.07	-1.36	-1.26	8.54	4.71	4.99	0.10

ZnTe	d	ε_{HOMO-1}	ε_{HOMO}	ε_{LUMO}	ε_{LUMO+1}	$\triangle_d$	$\triangle_{HOMO-LUMO}$	$\triangle_{HOMO-1-LUMO}$	$\triangle_{LUMO-LUMO+1}$
NR1	-15.10	-6.26	-5.78	-1.29	-1.11	8.84	4.49	4.97	0.18
NR2	-15.06	-6.13	-5.77	-1.31	-1.12	8.93	4.46	4.82	0.19
NR3	-15.05	-6.06	-5.77	-1.33	-1.15	8.99	4.44	4.73	0.18
NR4	-15.04	-6.01	-5.77	-1.33	-1.21	9.03	4.44	4.68	0.12
NR5	-15.03	-6.00	-5.77	-1.35	-1.25	9.03	4.42	4.65	0.10

Table 3: Valence excitation spectrum of the ZnS-NRs. Vertical excitation energy and corresponding oscillator strength are reported, along with the composition of the excited state. Among the low lying excitations, the first an those with $f > 0.1$ are shown Energies in eV and oscillator strengths in a.u.. Results obtained at PCM-B3LYP/def2-SVP//PBE/DZ.

ZnS							
	# Transition	E(eV)	f	Main Monoexcitations			Weight (%)
NR1	1	4.15	0.0968	HOMO	$\longrightarrow$	LUMO	72
				HOMO	$\longrightarrow$	LUMO+1	22
	7	4.89	0.3192	HOMO-4	$\longrightarrow$	LUMO	42
				HOMO-6	$\longrightarrow$	LUMO	24
	11	5.02	0.2246	HOMO-9	$\longrightarrow$	LUMO	40
				HOMO-6	$\longrightarrow$	LUMO	38
NR2	1	4.18	0.1174	HOMO	$\longrightarrow$	LUMO+1	44
				HOMO	$\longrightarrow$	LUMO	42
	2	4.64	0.6582	HOMO-1	$\longrightarrow$	LUMO	72
	8	4.77	0.6301	HOMO-3	$\longrightarrow$	LUMO	18
				HOMO-4	$\longrightarrow$	LUMO	18
				HOMO-1	$\longrightarrow$	LUMO	16
				HOMO-7	$\longrightarrow$	LUMO	12
NR3	1	4.17	0.1234	HOMO	$\longrightarrow$	LUMO+1	48
				HOMO	$\longrightarrow$	LUMO	24
				HOMO	$\longrightarrow$	LUMO+2	16
	2	4.59	0.8469	HOMO-1	$\longrightarrow$	LUMO	50
				HOMO-2	$\longrightarrow$	LUMO	18
				HOMO-2	$\longrightarrow$	LUMO+1	14
	3	4.65	0.6865	HOMO-2	$\longrightarrow$	LUMO	36
				HOMO	$\longrightarrow$	LUMO	22
				HOMO-1	$\longrightarrow$	LUMO	14
NR4	1	4.18	0.1295	HOMO	$\longrightarrow$	LUMO+1	44
				HOMO	$\longrightarrow$	LUMO+2	22
				HOMO	$\longrightarrow$	LUMO	16
	2	4.59	1.4501	HOMO-1	$\longrightarrow$	LUMO	42
				HOMO-2	$\longrightarrow$	LUMO	20
				HOMO-2	$\longrightarrow$	LUMO+1	18
	3	4.63	1.2945	HOMO-1	$\longrightarrow$	LUMO	30
				HOMO-2	$\longrightarrow$	LUMO	30
NR5	1	4.18	0.1438	HOMO	$\longrightarrow$	LUMO+1	38
				HOMO	$\longrightarrow$	LUMO+2	28
				HOMO	$\longrightarrow$	LUMO+3	12
	2	4.59	3.1135	HOMO-1	$\longrightarrow$	LUMO	58
				HOMO-2	$\longrightarrow$	LUMO+1	14

Table 4: Valence excitation spectrum of the ZnSe-NRs. Vertical excitation energy and corresponding oscillator strength are reported, along with the composition of the excited state. The first and the most intense transitions are shown for each rod. Energies in eV and oscillator strengths in a.u.. Results obtained at PCM-B3LYP/def2-SVP//PBE/DZ.

ZnSe							
	# Transition	E(eV)	f	Main Monoexcitations			Weight (%)
NR1	1	3.98	0.1135	HOMO	$\longrightarrow$	LUMO	68
				HOMO	$\longrightarrow$	LUMO+1	24
	7	4.62	0.5804	HOMO-4	$\longrightarrow$	LUMO	50
				HOMO-7	$\longrightarrow$	LUMO	28
NR2	1	3.99	0.1416	HOMO	$\longrightarrow$	LUMO	60
				HOMO	$\longrightarrow$	LUMO+1	42
				HOMO	$\longrightarrow$	LUMO+2	10
	4	4.39	0.8591	HOMO-3	$\longrightarrow$	LUMO	54
				HOMO-1	$\longrightarrow$	LUMO	24
NR3	1	4.00	0.1733	HOMO	$\longrightarrow$	LUMO+1	46
				HOMO	$\longrightarrow$	LUMO	26
				HOMO	$\longrightarrow$	LUMO+2	18
	2	4.33	1.7800	HOMO-1	$\longrightarrow$	LUMO	74
NR4	1	4.00	0.1883	HOMO	$\longrightarrow$	LUMO+1	42
				HOMO	$\longrightarrow$	LUMO+2	22
				HOMO	$\longrightarrow$	LUMO	18
				HOMO	$\longrightarrow$	LUMO+3	12
		4.31	2.8542	HOMO-1	$\longrightarrow$	LUMO	76
NR5	1	4.00	0.1966	HOMO	$\longrightarrow$	LUMO+1	38
				HOMO	$\longrightarrow$	LUMO+2	24
				HOMO	$\longrightarrow$	LUMO+3	12
				HOMO	$\longrightarrow$	LUMO	12
	2	4.29	3.7167	HOMO-1	$\longrightarrow$	LUMO	68

Table 5: Valence excitation spectrum of the ZnTe-NRs. Vertical excitation energy and corresponding oscillator strength are reported, along with the composition of the excited state. The first and the most intense transitions are shown for each rod. Energies in eV and oscillator strengths in a.u.. Results obtained at PCM-B3LYP/def2-SVP//PBE/DZ.

ZnTe							
	# Transition	E(eV)	f	Main Monoexcitations			Weight (%)
NR1	1	3.70	0.0844	HOMO	$\longrightarrow$	LUMO+1	72
				HOMO	$\longrightarrow$	LUMO	12
	16	4.36	0.2967	HOMO	$\longrightarrow$	LUMO+8	20
				HOMO-5	$\longrightarrow$	LUMO	20
				HOMO-8	$\longrightarrow$	LUMO	14
				HOMO-1	$\longrightarrow$	LUMO+1	10
NR2	1	3.70	0.0897	HOMO	$\longrightarrow$	LUMO+1	60
				HOMO	$\longrightarrow$	LUMO+2	20
	8	4.13	0.6214	HOMO-4	$\longrightarrow$	LUMO	40
				HOMO-1	$\longrightarrow$	LUMO	18
				HOMO-6	$\longrightarrow$	LUMO	10
NR3	1	3.71	0.1067	HOMO	$\longrightarrow$	LUMO+2	74
	4	4.05	1.4490	HOMO-1	$\longrightarrow$	LUMO	44
				HOMO-2	$\longrightarrow$	LUMO	22
NR4	1	3.70	0.1101	HOMO	$\longrightarrow$	LUMO+2	66
	3	4.03	3.5071	HOMO-1	$\longrightarrow$	LUMO	76
NR5	1	3.71	0.1180	HOMO	$\longrightarrow$	LUMO+2	58
				HOMO	$\longrightarrow$	LUMO+3	18
	3	4.00	4.8786	HOMO-1	$\longrightarrow$	LUMO	68

Table 6: Valence excitation spectrum of the ZnS-NSs. Vertical excitation energy and corresponding oscillator strength are reported, along with the composition of the excited state. Among the low lying excitations, the first an those with $f > 0.1$ are shown. Energies in eV and oscillator strengths in a.u.. Results obtained at PCM-B3LYP/def2-SVP//PBE/DZ.

ZnS							
	# Transition	E(eV)	f	Main Monoexcitations			Weight (%)
NS1	1	4.16	0.0421	HOMO	$\longrightarrow$	LUMO	92
	2	4.42	0.4451	HOMO-1	$\longrightarrow$	LUMO	92
	3	4.47	0.2277	HOMO-2	$\longrightarrow$	LUMO	56
				HOMO-3	$\longrightarrow$	LUMO	30
	4	4.50	0.1729	HOMO-3	$\longrightarrow$	LUMO	56
				HOMO-2	$\longrightarrow$	LUMO	28
	7	4.63	0.1402	HOMO-6	$\longrightarrow$	LUMO	44
	10	4.71	0.2371	HOMO-8	$\longrightarrow$	LUMO	40
				HOMO-7	$\longrightarrow$	LUMO	32
	12	4.79	0.1022	HOMO-10	$\longrightarrow$	LUMO	28
				HOMO-11	$\longrightarrow$	LUMO	20
	14	4.81	0.1627	HOMO-11	$\longrightarrow$	LUMO	26
				HOMO-10	$\longrightarrow$	LUMO	22
NS2	1	4.17	0.0361	HOMO	$\longrightarrow$	LUMO	76
	2	4.40	1.0049	HOMO-1	$\longrightarrow$	LUMO	79
	3	4.47	0.1965	HOMO-2	$\longrightarrow$	LUMO	33
				HOMO-4	$\longrightarrow$	LUMO	23
				HOMO-3	$\longrightarrow$	LUMO	20
	5	4.55	0.5597	HOMO-4	$\longrightarrow$	LUMO	51
	10	4.64	0.3900	HOMO-7	$\longrightarrow$	LUMO	42
				HOMO-8	$\longrightarrow$	LUMO	22
	13	4.68	0.1069	HOMO-10	$\longrightarrow$	LUMO	28
				HOMO-11	$\longrightarrow$	LUMO	22
	18	4.78	0.1077	HOMO-17	$\longrightarrow$	LUMO	34
NS3	1	4.39	1.3280	HOMO	$\longrightarrow$	LUMO	84
	2	4.44	0.3098	HOMO-1	$\longrightarrow$	LUMO	74
	4	4.48	0.9405	HOMO-3	$\longrightarrow$	LUMO	54
	5	4.50	0.1695	HOMO-4	$\longrightarrow$	LUMO	62
	8	4.60	0.6378	HOMO-6	$\longrightarrow$	LUMO	51
	9	4.60	0.1617	HOMO-7	$\longrightarrow$	LUMO	59
	10	4.63	0.2284	HOMO-11	$\longrightarrow$	LUMO	24
	17	4.67	0.1000	HOMO-13	$\longrightarrow$	LUMO	27
				HOMO-12	$\longrightarrow$	LUMO	24
	18	4.69	0.1221	HOMO-17	$\longrightarrow$	LUMO	40
	19	4.72	0.3307	HOMO-19	$\longrightarrow$	LUMO	44

Table 7: Valence excitation spectrum of the ZnSe-NSs. Vertical excitation energy and corresponding oscillator strength are reported, along with the composition of the excited state. The first and the most intense transitions are shown for each wire. Energies in eV and oscillator strengths in a.u.. Results obtained at PCM-B3LYP/def2-SVP//PBE/DZ.

ZnSe							
	# Transition	E(eV)	f	Main Monoexcitations			Weight (%)
NS1	1	3.82	0.0449	HOMO	$\longrightarrow$	LUMO	93
	2	4.02	0.4719	HOMO-1	$\longrightarrow$	LUMO	90
	3	4.04	0.3064	HOMO-2	$\longrightarrow$	LUMO	82
	7	4.25	0.1889	HOMO-6	$\longrightarrow$	LUMO	73
	9	4.33	0.1335	HOMO-7	$\longrightarrow$	LUMO	26
				HOMO-8	$\longrightarrow$	LUMO	20
	11	4.38	0.1550	HOMO-8	$\longrightarrow$	LUMO	58
				HOMO-7	$\longrightarrow$	LUMO	21
	16	4.48	0.3409	HOMO-13	$\longrightarrow$	LUMO	34
NS2	1	3.83	0.0398	HOMO	$\longrightarrow$	LUMO	79
	2	3.98	0.9807	HOMO-1	$\longrightarrow$	LUMO	73
	3	4.05	0.1888	HOMO-2	$\longrightarrow$	LUMO	47
	4	4.09	0.4261	HOMO-3	$\longrightarrow$	LUMO	41
	5	4.09	0.1412	HOMO-4	$\longrightarrow$	LUMO	61
	7	4.17	0.1170	HOMO-6	$\longrightarrow$	LUMO	70
	9	4.23	0.2212	HOMO-7	$\longrightarrow$	LUMO	38
	12	4.28	0.1440	HOMO-9	$\longrightarrow$	LUMO	32
	13	4.31	0.1308	HOMO-11	$\longrightarrow$	LUMO	24
				HOMO-10	$\longrightarrow$	LUMO	21
NS3	1	3.91	1.0659	HOMO	$\longrightarrow$	LUMO	84
	2	3.95	0.6319	HOMO-1	$\longrightarrow$	LUMO	81
	4	4.01	0.8026	HOMO-3	$\longrightarrow$	LUMO	69
	9	4.17	0.4697	HOMO-8	$\longrightarrow$	LUMO	58
	10	4.19	0.1971	HOMO-10	$\longrightarrow$	LUMO	46
				HOMO-9	$\longrightarrow$	LUMO	24
	12	4.23	0.2528	HOMO-12	$\longrightarrow$	LUMO	37
	16	4.27	0.5158	HOMO-15	$\longrightarrow$	LUMO	48

Table 8: Valence excitation spectrum of the ZnTe-NSs. Vertical excitation energy and corresponding oscillator strength are reported, along with the composition of the excited state. The first and the most intense transitions are shown for each wire. Energies in eV and oscillator strengths in a.u.. Results obtained at PCM-B3LYP/def2-SVP//PBE/DZ.

ZnTe							
	# Transition	E(eV)	f	Main Monoexcitations			Weight (%)
NS1	1	3.39	0.0434	HOMO	$\longrightarrow$	LUMO	91
	3	3.61	0.4011	HOMO-1	$\longrightarrow$	LUMO	78
	4	3.63	0.3805	HOMO-2	$\longrightarrow$	LUMO	60
NS2	1	3.39	0.0451	HOMO	$\longrightarrow$	LUMO	74
	3	3.61	1.1188	HOMO-1	$\longrightarrow$	LUMO	83
	4	3.65	0.5492	HOMO-2	$\longrightarrow$	LUMO	50
				HOMO-3	$\longrightarrow$	LUMO	35
	7	3.71	0.1520	HOMO-5	$\longrightarrow$	LUMO	43
				HOMO-4	$\longrightarrow$	LUMO	29
	11	3.80	0.1410	HOMO-7	$\longrightarrow$	LUMO	26
	14	3.84	0.1253	HOMO-8	$\longrightarrow$	LUMO	35
	15	3.84	0.1151	HOMO-9	$\longrightarrow$	LUMO	44
NS3	1	3.37	0.2895	HOMO	$\longrightarrow$	LUMO	41
				HOMO	$\longrightarrow$	LUMO+1	38
	2	3.48	0.9490	HOMO	$\longrightarrow$	LUMO	41
				HOMO-1	$\longrightarrow$	LUMO	24
	4	3.54	0.2287	HOMO-2	$\longrightarrow$	LUMO	55
	6	3.66	0.5662	HOMO-3	$\longrightarrow$	LUMO	55
	7	3.66	0.1332	HOMO-4	$\longrightarrow$	LUMO	62
	8	3.67	0.2003	HOMO-5	$\longrightarrow$	LUMO	31
	9	3.68	0.1456	HOMO-2	$\longrightarrow$	LUMO+1	24
	10	3.70	0.4947	HOMO-5	$\longrightarrow$	LUMO	22
	14	3.76	0.1370	HOMO-10	$\longrightarrow$	LUMO	<10
	15	3.77	0.4572	HOMO-12	$\longrightarrow$	LUMO	24
				HOMO-8	$\longrightarrow$	LUMO	23

Figure 1: TDDFT absorption spectra of the ZnS-NW1 at different levels, obtained by a Gaussian convolution the lowest 10 electronic transitions. The TDDFT absorption spectra calculated at PCM(water)-B3LYP/def2-SVP for the structures optimized at PBE/DZ and B3LYP/DZ differ only slightly, being the latter 0.05-0.10 eV redshifted with respect to the former. The spectra of the structure optimized with the COSMO representation of the solvent are consistently redshifted by only 0.10 eV as compared to the structure minimized *in vacuo*. For PBE, the spectra of the structures obtained in water and in acetonitrile are almost indistinguishable.

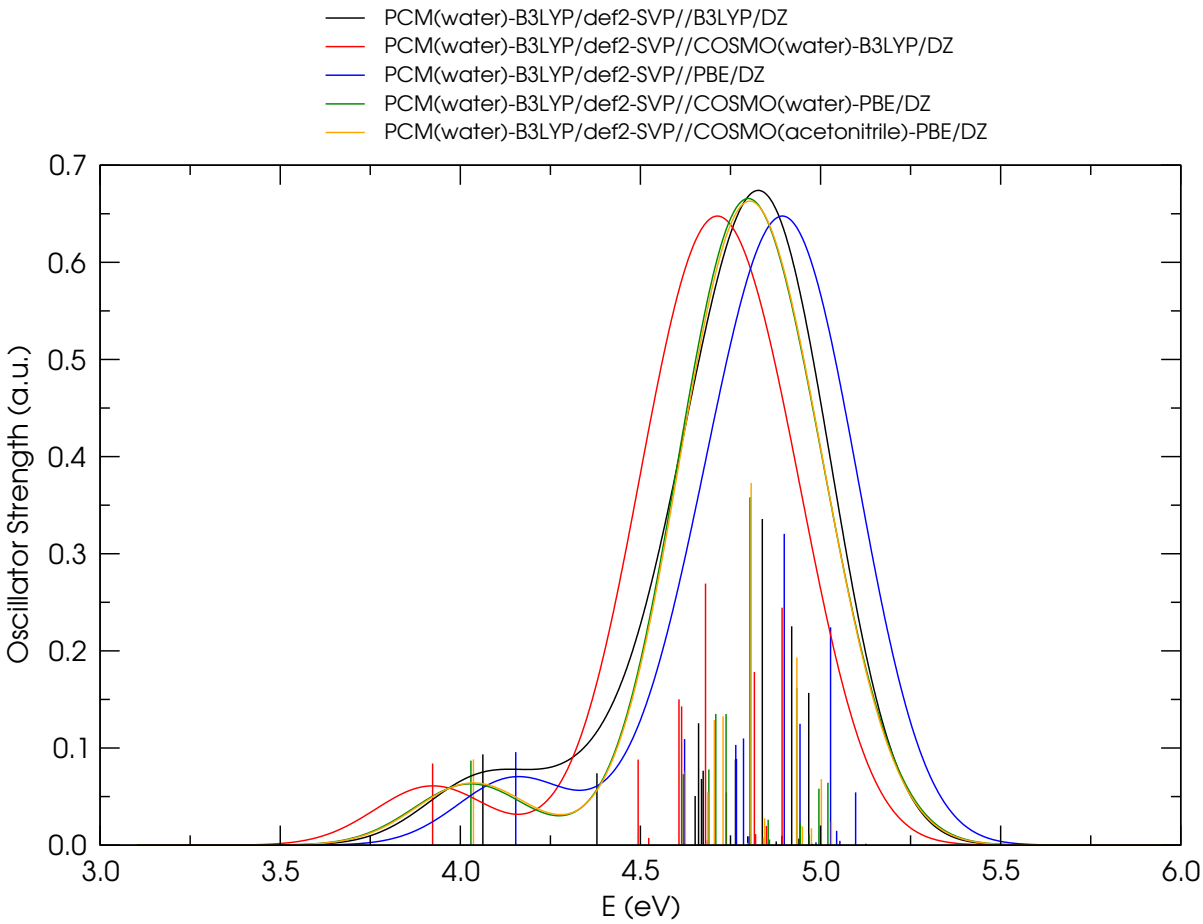

Figure 2: Geometrical structures of the optimized (a) ZnO-, (b) ZnS-, (c) ZnSe- and (d) ZnTe- QDs. In the case of the ZnO-QD, perspectives along the a, b and c crystallographic axes are shown. Light blue = Zn, red = O, yellow = S, orange = Se, green = Te and white = H atoms.

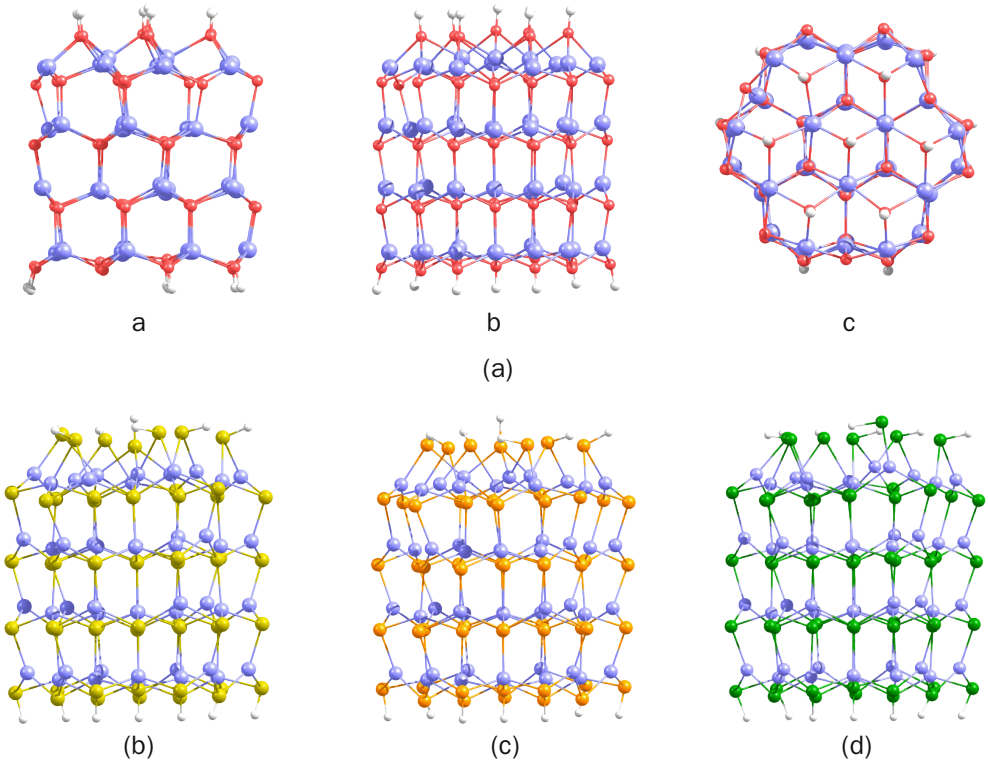

Figure 3: RDFs of the (a) ZnO-, (b) ZnS-, (c) ZnSe- and (d) ZnTe- QDs. The upper and the lower part of each panel show the structure of the optimized $(ZnX)_{48}(H_2X)_7$ QD and the unrelaxed $(ZnX)_{48}$, respectively. For sake of clarity, surface attached H_2X molecules have not been considered in the former.

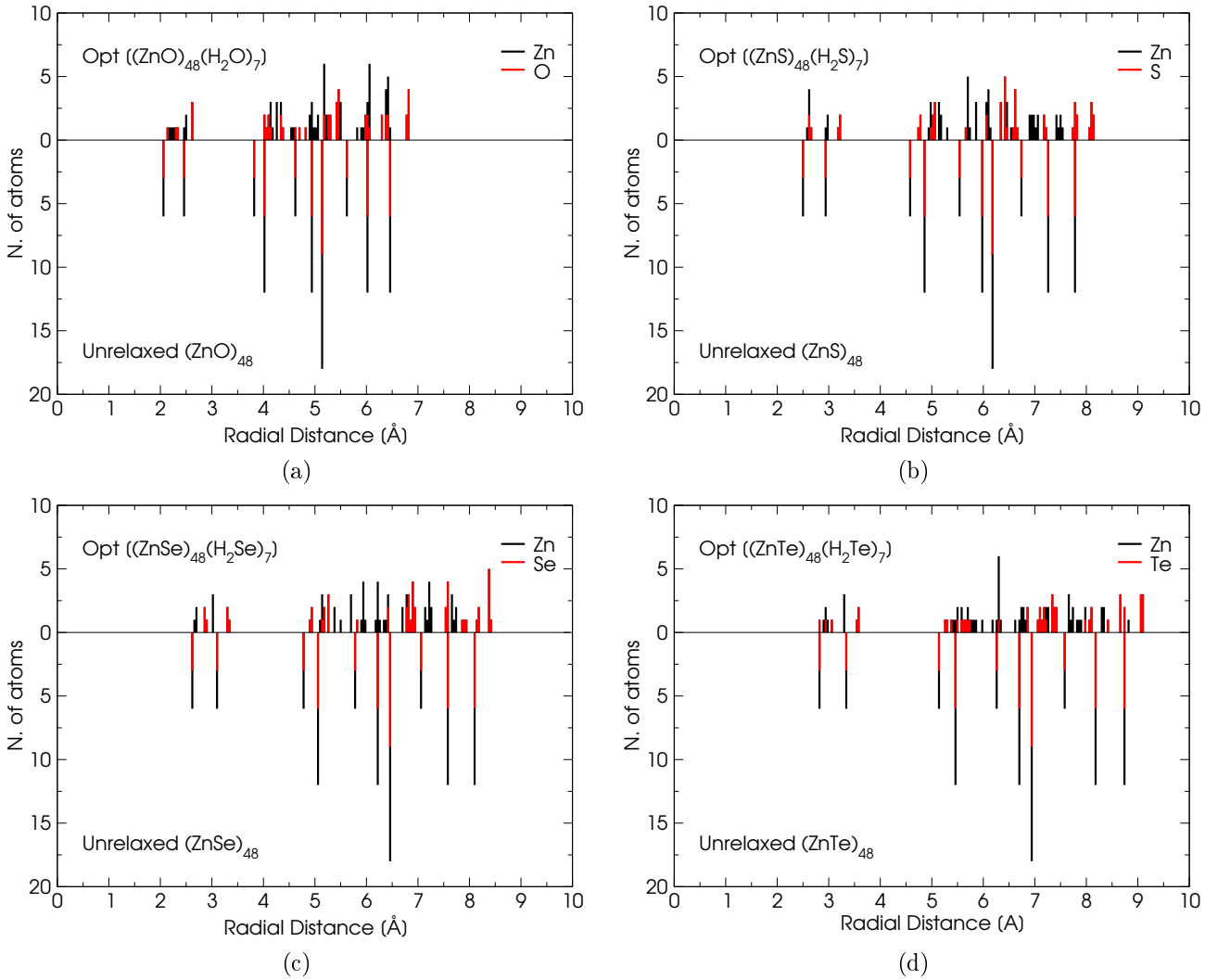

Figure 4: Density of States (DOS) of (a) ZnS-, (b) ZnSe and (c) ZnTe- NRs, obtained by a Gaussian broadening of $\sigma = 0.20$ eV of the individual Kohn-Sham orbitals. The insets show the detail of the electronic structure at the edges of the bandgap. Results obtained at PCM-B3LYP/def2-SVP//PBE/DZ.

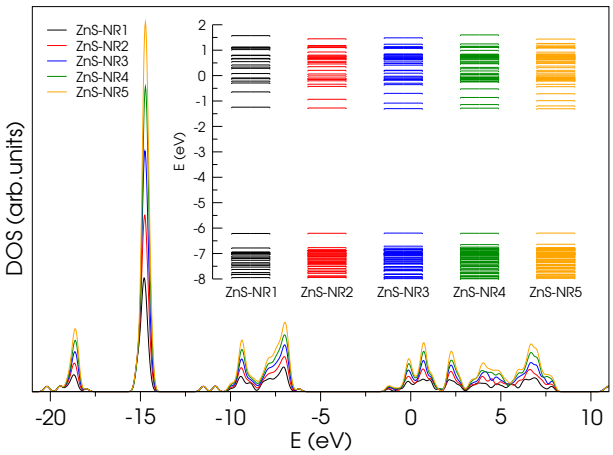

(a)

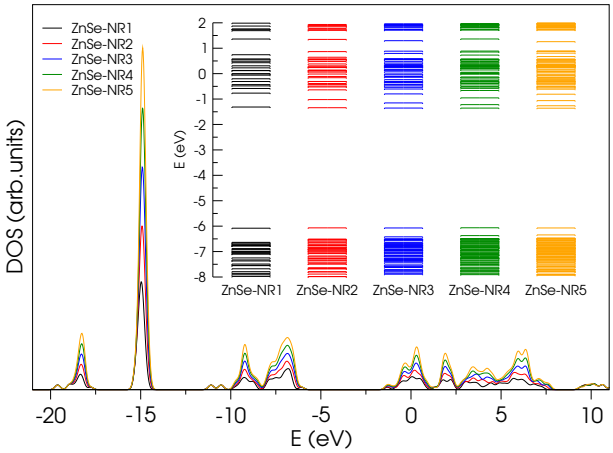

(b)

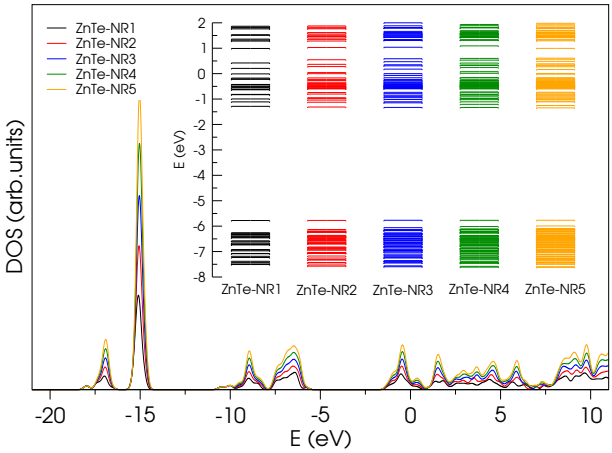

(c)

Figure 5: Optimized geometrical structures of the ZnS-NSs and isodensity plots of the HOMO-1, HOMO and LUMO. Light blue = Zn, yellow = S and white = H atoms.

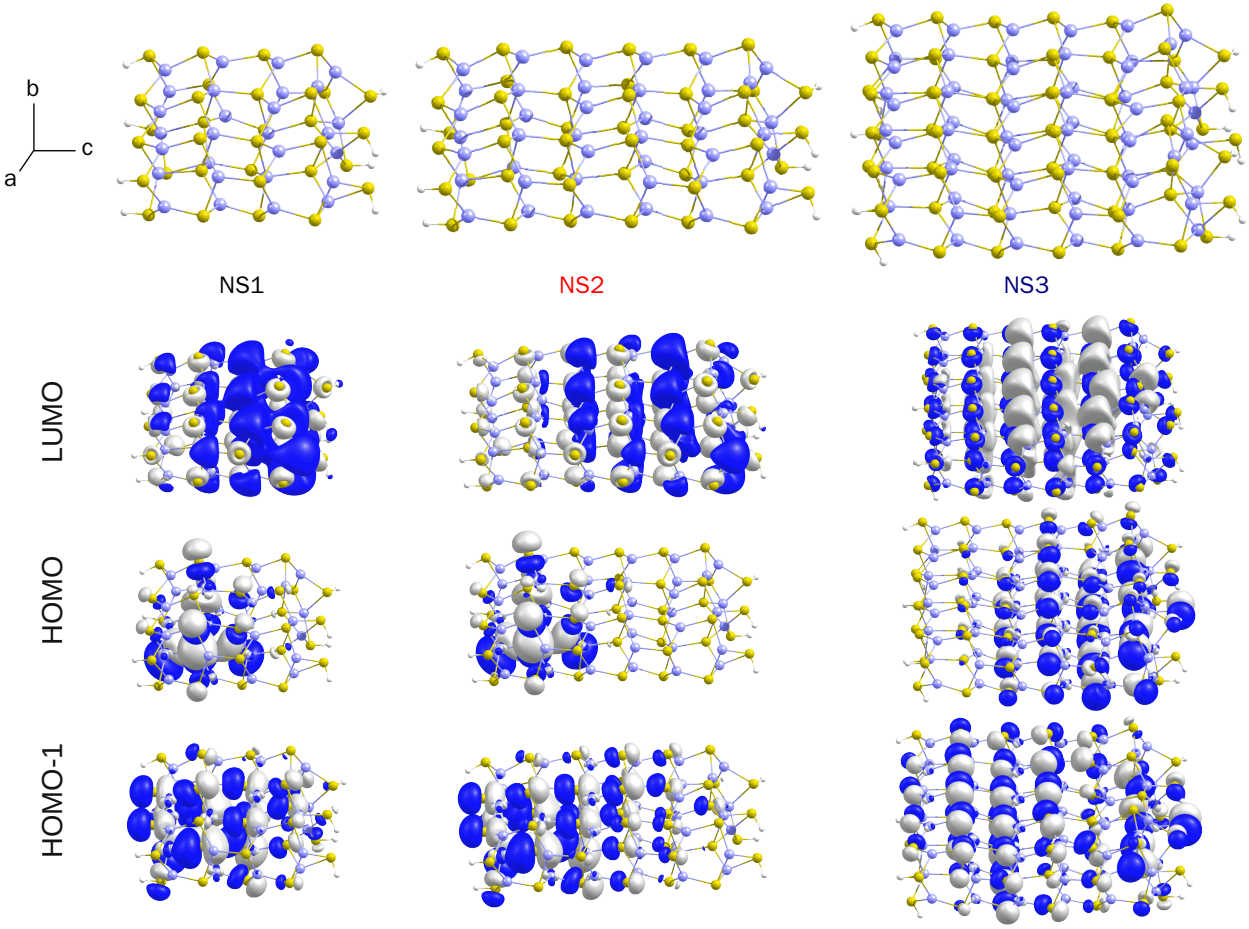

Figure 6: Density of States (DOS) of (a) ZnSe- and (b) ZnTe- NSs, obtained by a Gaussian broadening of $\sigma = 0.20$ eV of the individual Kohn-Sham orbitals. For NS1 and NS2 HOMO-1 has been chosen as VBM, given that HOMO is a midgap state. Results obtained at PCM-B3LYP/def2-SVP//PBE/DZ.

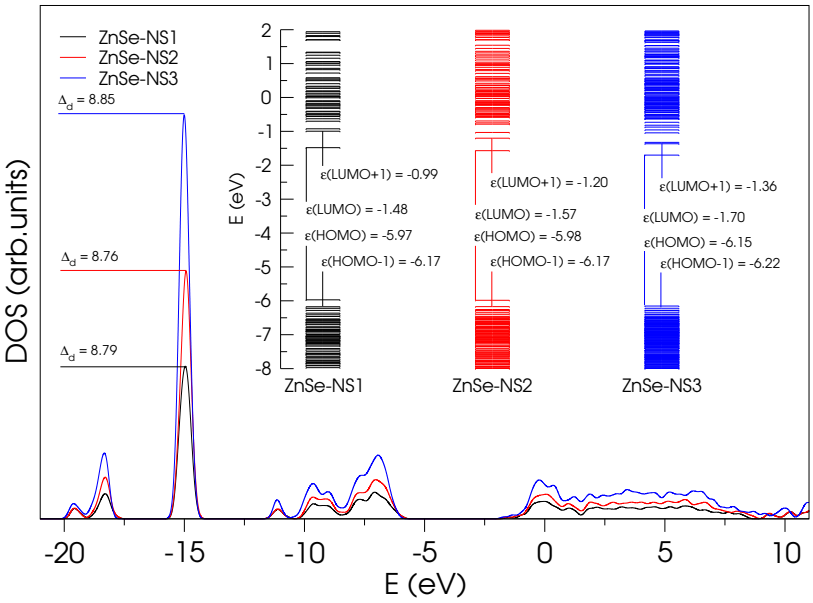

(a)

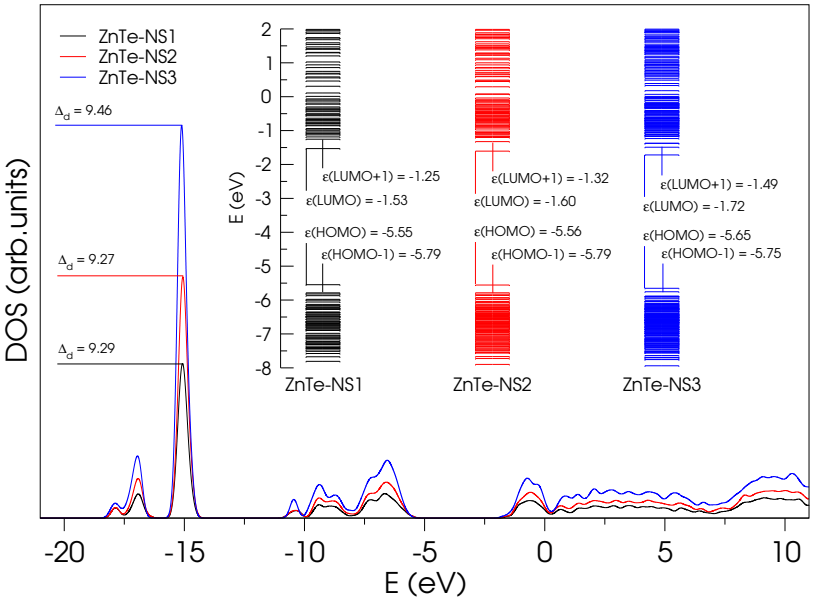

(b)

Figure 7: Calculated TDDFT absorption spectra for ZnSe-NSs, obtained by a Gaussian convolution with FWHM of 0.47 eV, calculated taking into account the lowest 20 excited states. Results obtained at PCM-B3LYP/def2-SVP//PBE/DZ.

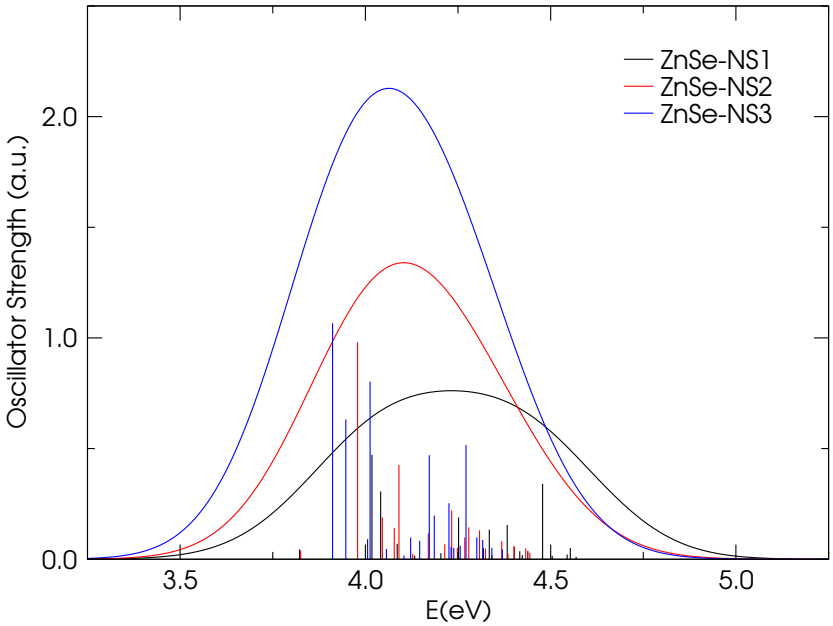

Figure 8: Calculated TDDFT absorption spectra for ZnTe-NSs, obtained by a Gaussian convolution with FWHM of 0.47 eV, calculated taking into account the lowest 20 excited states. Results obtained at PCM-B3LYP/def2-SVP//PBE/DZ.